Clouds and the Earth's Radiant Energy System (CERES)

Validation Document

Imager Clear-Sky Determination and Cloud Detection (Subsystem 4.1)

Patrick Minnis[1]
Louis Nguyen[1]
David F. Young[1]
Qing Z. Trepte[2]
Ronald M. Welch[3]
Bryan A. Baum[1]

[1]Atmospheric Sciences Division
NASA Langley Research Center
Hampton, VA 23681-0001

[2]SAIC
Hampton, VA 23666

[3]Department of Atmospheric Science
University of Alabama in Huntsville
National Space Science and Technology Center
Huntsville, AL 35805

August 2000

4.1.1 Introduction

4.1.1.1 Measurement and Science Objectives

This document describes a strategy for addressing the verification of cloud properties from EOS imager data, specifically clear-sky determination and cloud detection/masking. The methodology for this task is presented in Baum et al. (1995), Minnis et al. (1999a,b), and Trepte et al. (1999). CERES cloud retrieval algorithms have been developed using data from the Advanced Very High Resolution Radiometer (AVHRR, 1.1 or 4-km resolution at nadir), the High Resolution Infrared Radiometer Sounder (HIRS, 17.4-km resolution at nadir), various geostationary platforms such as the Geostationary Operational Environmental Satellite (GOES; 1-km visible, 4-km infrared), and, since 1998, the Tropical Rainfall Measurement Mission (TRMM) Visible-Infrared Radiometer (VIRS, 2-km resolution). Additional development will occur when new spectral channels are available from the Moderate Resolution Imaging Spectroradiometer (MODIS; 0.25, 05. and 1-km resolution) on the EOS satellites. While the CERES cloud detection algorithm was designed to function with input from any imager dataset, a number of questions remain as to how consistent the cloud retrievals are between the various imagers. Besides the differences in spectral channels between imagers, there are also differences in pixel resolution and time and angular sampling. In the following sections, a number of strategies are outlined, in order of priority, for verifying the horizontal cloud boundaries or cloud areal coverage. By contrast, the validation plan for section 4.2 considers the validation of cloud boundaries in the vertical dimension, i.e., with height. Examples of preliminary validations of the CERES analysis of VIRS data are shown.

4.1.1.2 Missions

The first launch of the CERES instrument was on the TRMM in late 1997. Operational analysis of CERES TRMM data began in January 1998. Another CERES package was launched on the EOS-AM-1 platform, Terra, in late 1999. It will be followed by another on the EOS-PM-1, Aqua. Follow-on missions to TRMM and EOS-AM and EOS-PM are currently planned. The CERES algorithms will be applied to data from MODIS on both Terra and Aqua.

4.1.1.3 Science data products

The cloud properties generated from imager data in CERES Subsystem 4.1, 4.2 and 4.3 will be convolved with CERES broadband radiometric data and saved in the CERES SSF product. The validation approaches outlined in this plan are primarily for the CERES Subsystem 4.1, cloud detection. However, the general approaches discussed here are similar to those used for the two remaining cloud subsystems and will not expanded much in the validation plans for those subsystems.

4.1.2 Validation Criterion

4.1.2.1 Overall approach

The validation strategy involves four key elements. Assessment of the calibration of the imager sensors relative to other standards is the first critical element for validating the dataset. The second element is visual quality control; the results, when displayed, should be consistent with a visual interpretation of the imagery. The third approach is to ensure that the retrieved clear-sky and cloud properties are consistent globally for both daytime and nighttime conditions. Finally, assuming that the clear-sky and cloud properties are consistent and reasonable on a global scale, the results should compare well with independent observations from ground-, air-, and other satellite-based observations.

The CERES cloud algorithms include a variety of input data that are used to predict clear-sky radiances, set thresholds, and retrieve parameters via comparison with theoretical models. In all of these steps, it is essential to have an assessment of the calibration of each channel used in the algorithm. Although the VIRS and MODIS carry onboard calibration systems, it is still necessary to compare the observed radiances to other sources to detect any gross errors in the onboard calibration, to determine if any long-term drift is occurring, and to quantify differences with other sensors used for cloud retrievals so that the relative effects of calibration differences between the CERES and other imagers on the cloud results can be quantified or normalized.

The inspection of raw imagery and the corresponding instantaneous clear-sky and cloud property maps, especially during the initial processing stages, is useful for detecting the most obvious problems. Because it is a subjective process, inspection is only a qualitative validation, but extremely useful. Some of the identified problems may be easily resolved, while others may be indicative of more subtle algorithm implementation errors. Data from each imager have idiosyncrasies that require some iterative analysis to understand. Software changes will be developed and implemented to account for those idiosyncrasies when possible.

Several methods are available for implementing steps to address the third key element. Proof of consistency may be found, for example, from inspection of global maps of derived clear-sky and cloud parameters, from comparison with previous results for some specified time period, or by comparison with other global clear-sky and cloud products such as the International Satellite Cloud Climatology Project (ISCCP), surface observation climatologies, or Clouds from AVHRR (CLAVR).Global, gridded clear-sky and cloud products may be generated automatically during processing. To some degree, comparison with time histories of previously generated results also may be automated. Comparison with other data sets such as ISCCP or CLAVR are more time intensive, especially concerning the interpretation of differences between various data sets (both different years and different sensors).

Once the behavior of the imager used to develop CERES clear-sky and cloud properties is understood and the retrieved clear-sky and cloud properties are consistent globally, comparison of cloud boundaries will be made with independent observations. Comparison of satellite-retrieved cloud properties with ground-based observations should be performed over a long time period for a number of regions, as discussed later in this document.

4.1.2.2 Sampling requirements and trade-offs

The satellite cloud cover retrievals will be organized according to recognized global cloud climatological regions and surface types because the sensitivity of a given algorithm depends on the background and cloud type. For example, cloud detection is much easier over a dark, uniform ocean surface than over bright, high contrast surfaces such as ice/snow and deserts. The following categories are used to facilitate validation of representative conditions:

a. Global cloud climatologies: There are 29 recognized cloud climatologies (Sherr et al. 1968) between 70N and 70S, as described in Table 1 (at end of this document). For each of the 40 global cloud climatologies, it is assumed that there are, on average, two surface types present. Therefore, there are a total of 40 * 2 * 3 *2 = 360 conditions (sunglint included). It is further assumed that 100 independent samples are necessary for each of these conditions, for a total of 36,000 samples. Many of these samples should include high spatial resolution Advanced Spaceborne Thermal Emission and Reflectance Radiometer (ASTER) global data for validation. For the ASTER validation data set, the number of samples can be reduced to 40 climatologies * 2 (day/night) * 100 independent samples = 8000 ASTER scenes (60 km x 60 km). ASTER has three visible channels, six near-infrared channels and five infrared channels. The spatial resolution of these channels is 15m, 30m and 90m, respectively. ASTER will be on the EOS-AM platform. Studies using ASTER would be similar to that of Minnis and Wielicki (1988) and Wielicki and Parker (1992), but extended to many of the cloud regimes where independent observations of cloud cover are sparse.

b. Surface types: ocean (tropics, midlatitude, and polar), vegetated land (tropics, midlatitude and polar, including tundra), non-vegetated land (deserts, other), mountains, snow-covered land (midlatitude and polar) and ice-covered water (sea ice and fresh water ice). A large number of 1° x 1° regions have been selected by the CERES team for intensive evaluation of all CERES products at the pixel level using visual inspection and, when possible, quantitative comparisons with more objective parameter determinations. A subset of those regions has been selected specifically for the CERES cloud subsystem. These 30 regions (Table 2) cover a wide variety of surface and cloud types and include some sites where intensive cloud-related measurements are taken regularly with ground-based instruments. A complete swath of imager data and pixel-level analysis results are produced and saved for each of these images so that the results can be evaluated in the context of the large-scale conditions. These regions also serve to account for the cloud climatological regions in Table 1.

c. Seasons: summer, winter and transitional.

d. Day/night: For cloud detection, the daytime algorithm is used for solar zenith angles (SZA) less than 82^{o}. For twilight conditions ($82° < SZA < 88°$), the nighttime algorithm is applied with some additional visible-channel reflectance checks. Sunglint is included in the daytime conditions.

4.1.2.3 Measures of Success

The CERES cloud retrieval algorithm determines whether each satellite imager (i.e., AVHRR, MODIS, VIRS) pixel is clear or cloudy with an indicator of whether the cloudy pixels contain single- or multiple-layered clouds and how confidently the identification is made (strong or weak descriptors). Other subclassifications are also used to categorize clear (noted below) and cloudy pixels with radiances that do not conform to the cloud property retrieval models ("no retrieval" descriptor). When the algorithms have matured, additional effort will be directed at determining sub-pixel fractional cloudiness. Until such algorithms are available, the goal of the CERES cloud mask is to obtain an accurate estimate of fractional cloudiness within a region using a classification of each pixel as 10% clear or cloudy only. The best accuracy estimate for current state-of-the-art clear-sky/cloud detection algorithms is on the order of 90%. The goal is 95% accuracy on a global basis.

The current clear-sky/cloud detection algorithms have been designed for specific regions, most notably polar, desert, regions of extensive biomass burning, and general global. Some previous global cloud masking algorithms, such as that used by CLAVR, generally have avoided sunglint regions. However, the present algorithms do not have this restriction. Optically thick clouds generally are detected with high accuracy over any surface, and most clouds are discriminated well for low brightness, low contrast water surfaces. However, thin cirrus clouds and sub-pixel scale cloudiness are much more difficult to identify, especially at night.

4.1.3 Pre- and Post-launch Algorithm Test/Development

4.1.3.1 Imager calibrations

The AVHRR sensors have a long history of calibration and normalization to each other and of use for continuous time series of cloud products (e.g., ISCCP). Other satellites, like the Geostationary Operational Environmental Satellites (GOES) have sensors have often been used to derive cloud properties (e.g., Minnis et al. 1995) and have been normalized to the AVHRR sensors (e.g., ISCCP). The second Along-Track Scanning Radiometer (ATSR-2) on the ERS-2 satellite has an onboard calibration system independent of either VIRS or MODIS. These satellite imagers and, perhaps, other imagers on aircraft and other satellites will be used to evaluate the relative and absolute calibrations of the relevant VIRS and MODIS channels. They may also be useful for estimating drift in any one of the VIRS or MODIS channels. The general approach to normalizing the sensors is to match the CERES imager swath with that from another satellite to within a tolerance of 15 min of the other satellite. The collocated pixels are then used to determine the calibration differences if the viewing zenith and relative azimuth angles differ by less than 10° and 15°, respectively. Generally, only data taken over ocean without sunglint are used to effect the normalizations. Because the GOES data are taken every 15 min, it is possible to obtain a large number of samples most easily by matching GOES images with those from either MODIS or VIRS.

Figure 1 shows a comparison of GOES-8 and VIRS pixels matched in this fashion from Nguyen et al. (1999). The GOES visible channel brightness counts are calibrated against the VIRS radiance. Using the known GOES-8 space count, the resulting slope is 0.83 compared to 0.80 for GOES compared with the NOAA-14 AVHRR. Thus, the VIRS and AVHRR gains are

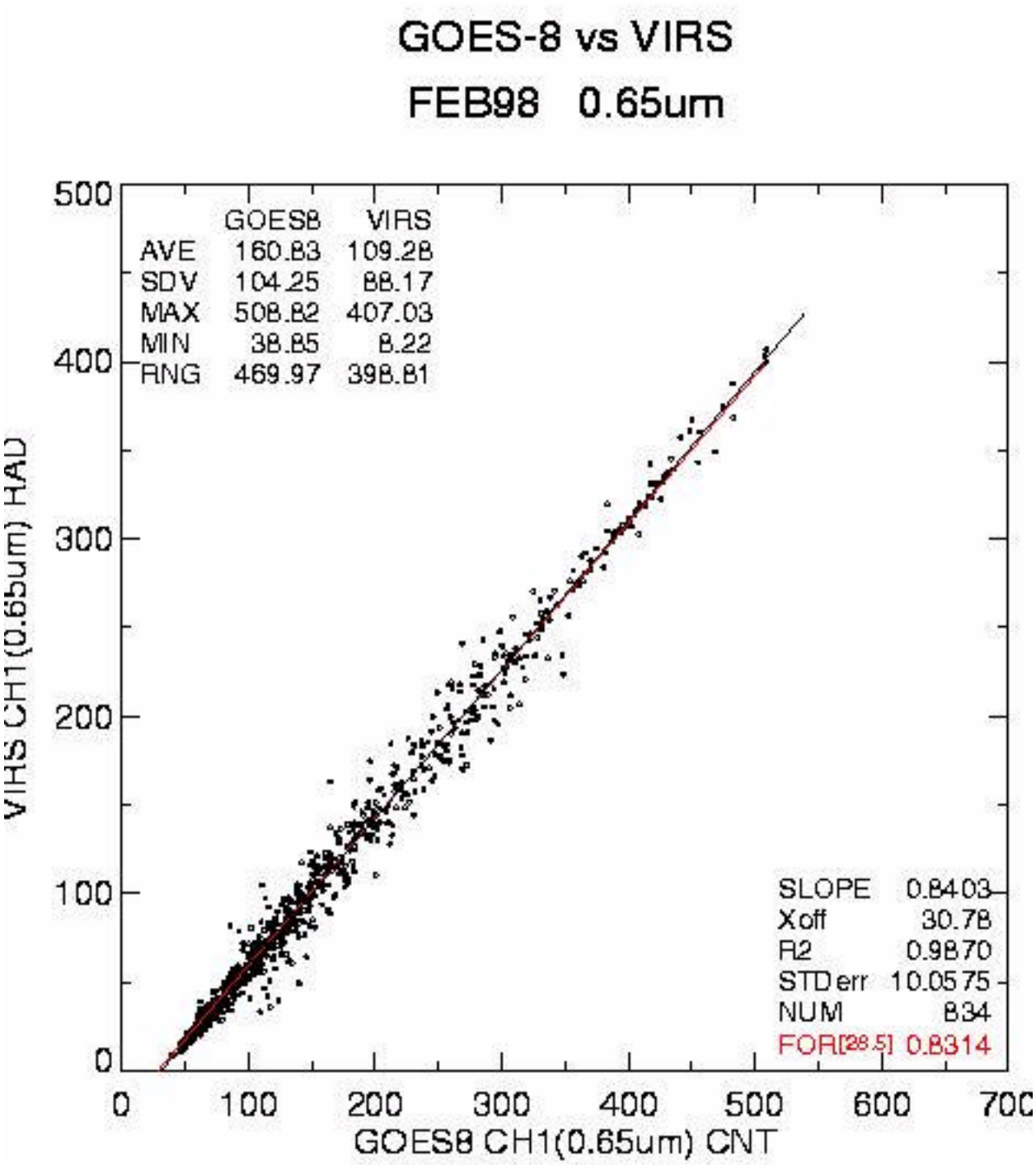

Figure 1. Scatterplot and regression fit of GOES-8 visible brightness counts and VIRS channel-1 radiance for collocated pixels averaged over a 0.5° region during February 1998.

within less than 4% of each other. The VIRS and MODIS data will also be compared to directly with AVHRR and ATSR-2 data and with each other when possible.

Another means for detecting calibration drift is by monitoring of the narrowband-to-broadband regression fit between convolved VIRS and CERES pixels using the visible and broadband short-

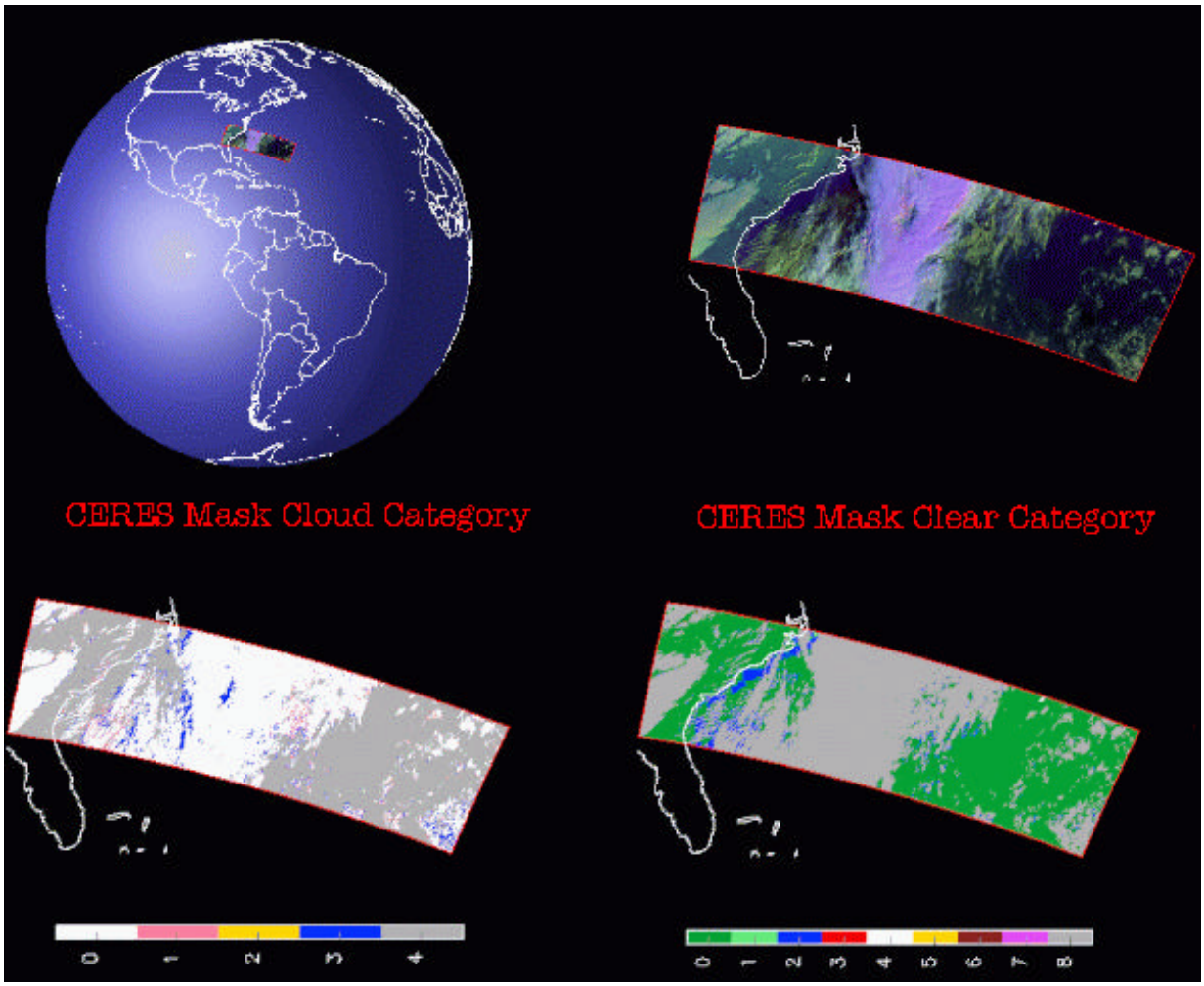

Figure 2. Example of VIRS imagery and results used to inspect quality of CERES cloud mask. Data taken at 1300 UTC, 9 January 1998.

wave (SW) channels, respectively, over ocean regions. The CERES SW channel calibration is maintained via periodic views of space and the solar disk. This approach assumes that the narrowband-broadband relationship is invariant with time over ocean regions when averaged over the globe. Initial results for the first 8 months showed no indication of drift in the VIRS channel-1 gain, but revealed a few calibration anomalies that have been corrected. This technique will continue with MODIS on both Aqua and Terra.

4.1.3.2 Visual inspections

A critical step in any retrieval process is to ensure that the derived fields are consistent with visual assessment of the imagery. This ongoing process is essential for all stages of the cloud analysis process, but is most important for the initial stage of detecting clouds within a given image. Figure 1 shows an example of a VIRS image extracted from an orbit and processed with the

CERES cloud mask for Cloud Validation Region 9. The upper left-hand image shows the global-context of the swath. The upper right-hand image is a 3-channel pseudo-color overlay using visible reflectance for red, 1.6-µm reflectance for green, and reversed-scale 11-µm brightness temperature for blue. This combination of colors facilitates recognition of different cloud and surface types in a single image. The cloud categories in the lower left denote the final classification of the cloudy pixels as strong clouds (0), weak clouds (1), no-retrieval clouds (2), or no clouds (3). The lower right-hand picture denotes the final classification for the clear pixels as strong (0), weak (1), smoke (2), fire (3), snow (4), glint (5), shadow (6), aerosol (7), or not clear (8).

When obvious discrepancies between the imagery and classifications are detected, the case can be more thoroughly examined using images of the input parameters, including individual spectral images, differences between the observed and expected clear-sky values, and other variables that may help determine why the discrepancies occurred. The code or input values may then be modified to minimize the discrepancy. Whenever the algorithm or input values are changed, results from other scenes are examined to ensure that the alteration did not adversely affect them. Other problems that can be detected through visual inspection of instantaneous results include day-to-night changes in the derived cloud properties, dramatic changes in properties over a given area from examination of two successive overpasses, and dramatic changes in the properties at the interface between two surface types (e.g., coastline). If the code cannot be altered to eliminate any of the identified problems, then the type of problem encountered and an estimate of its frequency are included, as part of the validation process, in the CERES Data Quality Summary for the relevant subsystem, so that users of the results will be aware of any recognized errors.

4.1.3.3 Consistency and global comparison studies

The second step in the process of verification is to ensure that the mean cloud properties are consistent on a global scale for both daytime and nighttime cases. Additionally, any dependence of the cloud fraction on background or viewing and illumination angles should also be determined and understood. Figure 3 shows a comparison of zonal mean cloud amounts derived from surface observations (Hahn and Warren 1999) for all Julys during a 22-year period and from VIRS data taken during July 1998. The zonal patterns are very similar, especially in the northern hemisphere where surface observations are more representative of the entire zone. In the southern hemi-.sphere, there are few observations in the Pacific Ocean. While there are discrepancies in the location of the southern hemisphere minimum, thee mean cloud amounts differ by only 0.5% overall. Complete agreement between the two datasets is not expected because of sampling, temporal, and viewing perspective (e.g., Minnis et al., 1995) differences. Nevertheless, it may be concluded that the VIRS results for this month are reasonable because they are close in magnitude and zonal distribution to previous climatologies. Similar comparisons should be performed for data from all months and for MODIS results as well. Data from other sources like ISCCP should be compared to the CERES cloud amounts also to determine how well they fit into other satellite cloud climatologies. Spatial distributions and day time and nighttime averages of CERES cloud amounts should also be compared with their climatological counterparts to determine if there are problems over particular surface types or time of day.

The VIRS viewing zenith angle (VZA) ranges between 0 and 48°, while the MODIS VZA extends to nearly 70°. For a given region, the VIRS can view nearly all times of day and, hence, can measure a cloud property at nearly all possible SZA's. MODIS can only observe the same

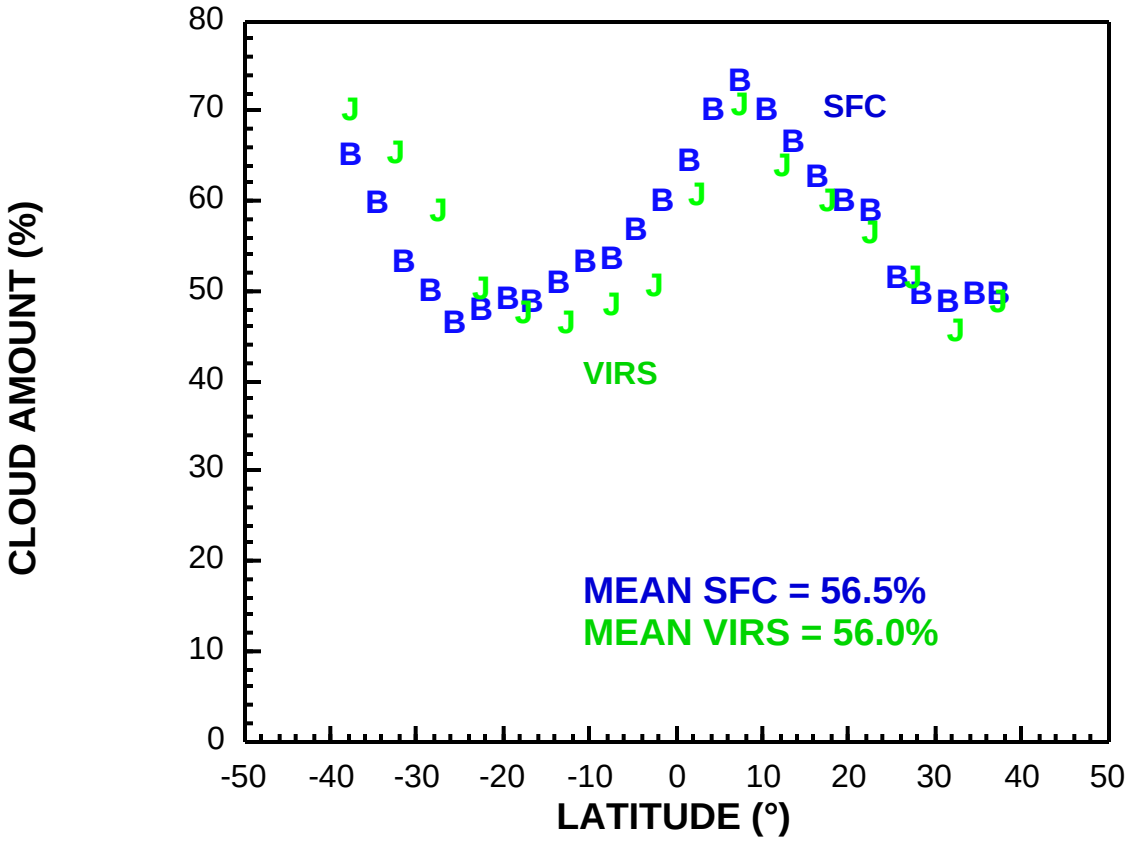

Figure 3. Comparison of mean July cloud amounts from surface observations (1971-1992) and from preliminary CERES cloud mask applied to VIRS data taken during July 1998.

region only over a limited SZA range because of its Sun-synchronous orbit. The thresholds used to detect clouds are sensitive to the viewing and illumination conditions because of the anisotropy of the reflectance field from a given Earth surface type and structure. Thus, some variation is expected to occur. To be able to account for the dependencies on viewing and illumination angles, the cloud properties, including cloud fractional coverage, should be averaged over the various viewing and illumination conditions for various surface types and times of day.

Figure 4 show examples of mean VIRS-derived cloud fractions for July 1998 averaged over VZA and relative azimuth angle (RAZ). The average cloud amount increases by 4% between 0 and 48° VZA angle over both land and water. This variation is similar to that seen by Minnis (1989) using a different dataset and thresholding procedure. Over land, more cloudiness is detected in the forward and backward scattering directions than at cross-scattering directions. The variation of cloud amount with RAZ over water shows a slight minimum in the forward scattering direction, but is negligible for RAZ > 50°. This ocean minimum may be due to less cloud detection in sunglint than in non-glitter conditions. The variation over land may be arise from inadequate characterization of clear-sky reflectance for some land types or to some unique relationships between RAZ and the location on Earth. More months of data may need to be averaged together to minimize such sampling effects. From these initial results, it is clear that the angular effects must be characterized using many different data selection criteria.

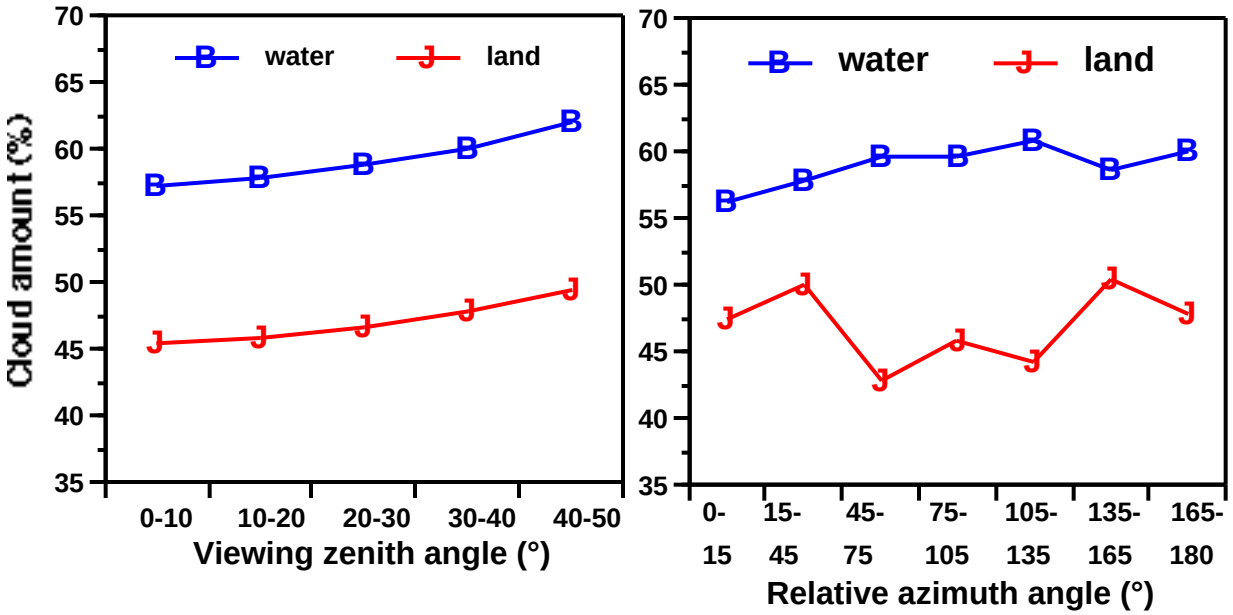

Figure 4. Mean cloud amounts as a function of VZA and RAZ from VIRS for July 1998 using a preliminary CERES cloud mask.

4.1.3.4 Direct comparisons with simultaneous independent observations

To validate beyond reasonableness and to better determine which set of angular conditions produce the "best" cloud amount, it necessary to quantify the differences with observations that can be assumed to constitute cloud truth. Such comparisons must be conducted carefully because of significant spatial and temporal differences between the various observing systems. For instance, it is important to account for the relatively small size of the lidar or radar field-of-view (FOV), as compared to the much larger satellite FOV. Also, lidars and radars may retrieve different cloud boundaries, depending upon their sensitivity to cloud effective particle size, optical depth, etc. Differences between remotely-sensed and ground-based estimates of cloud cover must be examined carefully without automatically assuming that only one value is correct. Similar cautions apply to surface observer estimations of cloud cover. Surface observers have a very different FOV. Cloud sides are observed not only by surface observers but also by the satellite sensors at the larger observing angles. Therefore, estimates may be differentially biased, depending upon cloud thickness.

4.1.3.4.1 ARM sites

The highest priority set of observations will be those where CERES cloud properties can be compared *routinely* to those obtained at a well-known surface site such as that provided by the Atmospheric Radiation Measurement program. Extended observations will be provided by the ARM sites, but not at all the locations required according to the categories above. These include the Southern Great Plains site (central Oklahoma, Table 2, #7), the Tropical West Pacific sites(cur-

rently Manus and Nauru Islands, #27 and 28), and the Arctic site (north slope of Alaska, #30). The CERES results can be compared to data from these sites over all seasons for a long time period in different cloud regimes. Cloud fraction can be measured several different ways at these sites using visual observations, whole-sky imaging cameras, radar, and lidar. Thus, a range of spatial dimensions and objectivity can be used to assess the uncertainties in the surface observations relative to the satellite-derived values. The comparison of visual and radar or lidar observations at these sites is especially important because the active sensors are unavailable at most other locations where visual observations are taken. Differences between the visual and radar-based observations are expected (Minnis et al. 2000), so it is important they be understood to put the comparisons with the larger network (see below) in perspective. The small number of well-equipped sites imposes some limitations on the validation process. If algorithms are developed or tuned specifically to improve retrievals in one region, problems may occur in different regions. Thus, the validation with data taken at other locations is important.

4.1.3.4.2 Surface observers

Cloud fraction can be verified over more climate regimes and backgrounds by using the surface weather station reports collected by the NOAA National Meteorological Center (NMC). The NMC surface synoptic observations include cloud fraction (in octals) as well as information about cloud types and cloud layering. Besides surface synoptic observations, there is also an effort to compare ground observations of cloud cover with satellite observations using an Automated Surface Observing System (Schreiner et al. 1993) over the continental United States.

Surface observations have long been used for assessing satellite-derived cloud amounts. Minnis and Harrison (1984) compared cloud amounts derived from GOES over 2.5° regions to those observed from surface sites in North America and the adjacent oceans. They found that the satellite generally detected fewer clouds in the tropics (small VZA), but agreed well, on average, with ship-based observations in the mid-latitudes. The results over land were mixed with a mean underestimate of 5%. In a more detailed study, Minnis et al. (1995) found that the optimal scale for comparing surface visual observations with satellite-derived cloud amounts was around 90 km. Thus, cloud amounts should be averaged for a nominal 1° latitude -longitude box centered on the observer's site. Rossow et al (1993) reported that surface observations agreed with ISCCP cloud amounts to within 15% rms with average biases of only a few percent. The biases and rms errors, however, varied considerably with cloud type and background. For example, cloud amounts over land underestimated the cloud cover by about 10% (somewhat less in summer and somewhat more in winter), but were approximately correct over oceans. Similar comparisons of the CERES cloud cover retrievals will be performed using instantaneous matched surface datasets. The ultimate objective is to understand and eventually minimize the biases for all surface and cloud types. More comparisons will be conducted when coincident data from other satellite cloud projects (e.g., MODIS, ISCCP, CLAVR) become available.

The input datasets used by CERES will also be examined and updated by comparison with other sources (e.g., downlooking pyrgeometer data at ARM sites or skin temperatures derived with microwave imagers) and with actual observations by VIRS and MODIS. Clear-sky maps of albedo and surface emissivities were generated from ISCCP data for the initial CERES cloud detection algorithms. These were updated by analysis of high-resolution AVHRR and VIRS data. The updated maps are used in the final CERES cloud algorithms. European Center for Medium

Range Weather forecasting (ECMWF) soundings and skin temperatures are used with the surface emissivities to predict clear-sky temperatures for each location observed during a given overpass. Differences between these input data and the clear-sky observations will be computed to assess the input values and determine corrections if necessary. Such differences will also be useful for improving the ECMWF predictions of skin temperature and the empirical surface emissivities.

The clear-sky temperatures and reflectances also depend on the atmospheric absorption computed for each channel. For channels, especially infrared, affected by water vapor absorption, the humidity and temperature profiles from the ECMWF are critical input. To determine the uncertainties in the clear-sky temperatures introduced by the atmospheric parameters, balloon soundings will be used to determine instantaneous errors in the temperature and humidity profiles, and consequently, the predicted temperatures. These comparisons are especially critical over remote areas where radiosonde data are not used as input for the ECMWF analyses. For that reason, these soundings will generally be available only during special field programs (see below).

4.1.3.4.3 Regional (short-term) comparison of CERES with ground-based observations

A number of field programs have addressed various aspects of cloud property retrieval. Instrumentation for these campaigns varies widely. It is only recently that radars have begun to complement lidars to determine cloud boundaries. Past (e.g., FIRE, SCAR, SHEBA, TOGA-COARE, CEPEX, ASTEX, ECLIPS, MCTEX, NAURU99, and TARFOX) and future field experiments (SAFARI, CRYSTAL, CLAMS, and others) will provide important validation data for their particular climatic and background conditions; however, validation samples over mid-latitude mountains, deserts, and tropical land should be included in future experiments. For prelaunch experiments, the exact VIRS and MODIS channels (spectra and resolution) will be unavailable for comparison. Thus, the algorithms will be tested using surrogate satellite (AVHRR, GOES, ATSR-2, etc.) data in those cases. For post-launch experiments, the VIRS and MODIS data as well as the surrogate imagers should be used in the validation comparisons to distinguish between the results from each of the imaging systems so that the prelaunch results may be interpreted relative tot he expected performance of VIRS and MODIS.

The surface observations taken during these experiments are often similar to those taken regularly at the ARM sites. Thus, the same types of comparisons will be conducted for satellite overpasses to obtain the cloud amount validations in areas where long-term observations are unavailable

4.1.3.4.4 Aircraft comparisons

Comparisons of satellite and ground-based observations will lead to significant deficiencies in particular regions. These regions include: polar, desert, mountains, coastal, and regions of biomass burning. In some of these regions the AVIRIS and MAS data may be used to improve and validate the algorithms. Thin cirrus may be detected using the 1.38um channel of both AVIRIS and MAS. MAS data taken over the Beaufort Sea and in Brazil will be used for the polar and biomass burning regions. And, AVIRIS data taken during the FIRE and ASTEX experiments will be used over land and ocean surfaces. Additional data taken during upcoming field experiments will be used in a similar fashion.

4.1.3.5 Operational surface networks

The following products are likely to be used in pre-launch activities:

1. National Weather Service (NWS) global synoptic cloud observations
2. Ceilometer network (limited to continental U.S.)
3. Blended Analysis sea surface temperatures
4. COADS data set
5. Surface observer 3-h reports
6. DOE ARM data
7. Automated Surface Observing System

4.1.3.6 Existing satellite data

A list of the satellite data sets used in pre-launch activities are:

1. AVHRR
2. HIRS
3. GOES-8 and GOES-9
4. ISCCP cloud climatologies
5. CLAVR cloud climatologies
6. ATSR-2
7. MAS and AVIRIS aircraft data

4.1.4 Additional Post-launch Activities

4.1.4.1 Planned field experiments and studies

The same approach as presented in Section 4.1.3.1 will be followed for post-launch activities. Since the cloud retrieval properties for the imager data are not going to be saved as an actual data product, selected regions will be saved daily for validation activities (Table 2). The list of selected regions includes both poles, North and South America, the coasts of Europe, persistent stratus regimes, the Tropical DOE ARM site and northern Australia, and a few other specific regions. These subsetted data sets will be produced through the Langley DAAC, and detailed analysis will be conducted primarily by the CERES Co-Investigators.

4.1.4.2 Other EOS-targeted coordinated field campaigns

With the comparison of satellite and ground-based observations of cloud boundaries/ cloud cover, according to the strategies previously outlined, deficiencies will still exist over midlatitude oceans, mountains, deserts, polar regions and tropical land, especially in regions of heavy biomass

burning. To fill data-sparse gaps in the imager sampling, it would be beneficial to plan field campaigns for these areas, or to join already planned field campaigns.

4.1.4.3 Needs for other satellite data

ASTER high spatial resolution data will be utilized for global cloud cover validation. As described in Section 4.1.2.2, ASTER data will be acquired for the 40 global cloud climatologies. A total of 100 independent samples are required for each of the 40 climatologies and both for day and night, for a total of 8000 scenes (60km x 60km). It will be necessary to arrange with the ASTER team to acquire the data consistent with their duty cycle. While the ARM sites and NOAA NMC surface synoptic observations will provide long-term, stable data sets for validation, (see section 4.1.2.2) many cloud climatological regimes, especially over ocean and near the poles, cannot be validated with surface observations. To fill in the gaps, ASTER/MODIS comparisons will provide some insight as to how the CERES algorithms are working, much like the current LANDSAT studies (e.g., Wielicki and Parker 1992), in regions where surface observations are sparse.

Another very useful set of satellite measurements for validation purposes would be lidar/radar observations, such as PICCASSO-CENA and CloudSat. The former will have a cloud and aerosol detecting lidar, while the latter will carry a cloud-detecting radar. These satellites are scheduled for launch in 2002 and will fly in tandem with one of the EOS satellites. Data from the other satellites used in the pre-launch validation should also be used for comparisons with the EOS results.

4.1.4.4 In-situ measurement needs at calibration/validation sites

The ideal set of instruments at the surface sites include a downlooking pyrgeometer and infrared window (10-12 μm) radiometer, a cloud lidar, a cloud radar, a laser ceilometer, a digital whole sky imager (WSI) system, a trained visual observer, regular radiosonde launches, and a narrowband solar system for measuring surface albedo at MODIS wavelengths. At present, the ARM sites have the most comprehensive set of instruments in this list.

4.1.4.5 Intercomparisons (multi-instrument)

Cloud amounts from WSI, surface observers, and radar/lidar systems should be compared to estimate the uncertainty in these validation sets. Similarly, cloud fractions measured with collocated VIRS and MODIS data should be compared to determine the robustness of the algorithms, verify angular dependence derived from one satellite, and to determine the effects of satellite resolution on the derived values.

4.1.5 Implementation of validation results in data production

4.1.5.1 Approach

The validation of clear-sky radiances, cloud detection and cloud property retrievals will take place at the CERES SCF or at the investigator home institutions. While some of the global mapping functionality can be automated, most of the effort described in this document requires interaction with an investigator. The investigators will need ready access to cloud boundary information from each of the ARM sites, to other sites that are operationally providing cloud boundary information, to the ASTER cloud masks, as well as to the subsetted data sets of retrieved cloud properties. NOAA NMC synoptic observations should be acquired in a timely fashion and in a standard format such as HDF.

4.1.5.2 Role of EOSDIS

EOSDIS will have an important but limited role in this process. For the retrieved cloud parameters listed in Table 4.4-4 of the CERES Subsystem 4.4, entitled "Convolution of imager cloud properties with CERES footprint point spread function," the volume of one hour of processed imager data is approximately 600MB. These retrievals are not a data product, but they are subsequently convolved with CERES footprints. It would be impractical to save all of the output from processing each hour of imager data. Rather, the output data stream will be subsetted to include only a select number of regions around the globe that are useful for validation purposes.

The data center responsible for processing CERES data should be tasked to routinely save the data from the prescribed set of regions designated by the CERES team. The saved data should be considered to be a temporary data product. Cloud boundary data from the sources listed in this document also should be available from and saved by EOSDIS.

4.1.5.3 Plans for archival of validation data

The set of CERES subsetted regions, corresponding ASTER imager data, surface observational data and aircraft data all should be saved on DAT or Exabyte tape and be provided to investigators for analysis at their SCFs.

4.1.6 List of Acronyms

ARM	Atmospheric Radiation Measurement Program
ASTER	Advanced Spaceborne Thermal Emission and Reflectance Radiometer
ASTEX	Atlantic Stratocumulus Transition Experiment
ATSR-2	Along-Track Scanning Radiometer
AVHRR	Advanced Very High Resolution Radiometer

CENA	Climatologie Etendue des Nuages et des Aerosols
CLAMS	Chesapeake Lighthouse and Aircraft Measurements for Satellites
COADS	Comprehensive Ocean-Atmosphere Data Set
CRYSTAL	Cirrus Regional Study of Tropical Anvils and Cirrus Layers
DAAC	Distributed Active Archive Center
DOE	Department of Energy
ECLIPS	Experimental Cloud Lidar Pilot Study
ECMWF	European Center for Medium Range Weather Forecasting
ERS-2	Environmental Resources Satellite
FIRE	First ISCCP Regional Experiment
GOES	Geostationary Operational Environmental Satellite
HIRS	High-resolution Infrared Radiometer Sounder
ISCCP	International Satellite Cloud Climatology Experiment
LITE	Lidar in Space Technology Experiment
MAS	MODIS Airborne Simulator
MODIS	Moderate resolution Imaging Spectrometer
NAURU99	Nauru Island ARM Experiment in 1999
NMC	National Meteorolgical Center
PICASSO	Pathfinder Instruments for Cloud and Aerosol Spacebourne Observations
SAFARI	South African Regional Science Initiative
SHEBA	Surface HEat Budget in the Arctic
TARFOX	Tropospheric Aerosol Radiative Forcing Observational Experiment
TRMM	Tropical Rainfall Measuring Mission
VIRS	Visible and Infrared Scanner

4.1.7 References

Baum, B. A., R. M. Welch, P. Minnis, L. L. Stowe, J. A. Coakley, Jr., and co-authors, 1999: Imager clear-sky determination and cloud detection (Subsystem 4.1). “Clouds and the Earth’s Radiant Energy System (CERES) Algorithm Theoretical Basis Document, Volume III: Cloud Analyses and Radiance Inversions (Subsystem 4)”, *NASA RP 1376 Vol. 3*, edited by CERES Science Team, December, 43-82.

Hahn, C.J., and S.G. Warren., 1999: Extended Edited Synoptic Cloud Reports from Ships and Land Stations Over the Globe, 1952-1996. *NDP026C*, Carbon Dioxide Information Analysis Center, Oak Ridge National Laboratory, OAK Ridge, TN.

Minnis, P., 1989: Viewing zenith angle dependence of cloudiness determined from coincident GOES East and GOES West data. *J. Geophys. Res.*, **94**, 2303-2320.

Minnis, P., D. R. Doelling, V. Chakrapani, D. A. Spangenberg, T. Uttal, R. F. Arduini, and M. Shupe, 2000: Cloud coverage during FIRE ACE derived from AVHRR data. In press, *J. Geophys. Res.*, August.

Minnis, P. and E. F. Harrison, 1984: Diurnal variability of regional cloud and clear-sky radiative parameters derived from GOES data, Part I: Methodology. *J. Climate Appl. Meteor.*, **23**, 998-1011.

Minnis, P., W. L. Smith, D. Garber, J. K. Ayers, and D. R. Doelling, 1995: Cloud properties

derived from GOES-7 for the Spring 1994 ARM Intensive Observing Period using version 1.0.0 of the ARM satellite data analysis program. *NASA RP 1366*, August, 59 pp.

Minnis, P., Young, D. F., Spangenberg, D. A., Heck, P. W., D. R. Doelling, Q. Trepte, and Y. Chen, 1999a: Cloud mask for CERES from VIRS on the TRMM satellite. *Proc. ALPS 99 Conference*, Meribel, France, January 18-22, **WK-P-06**, 1-4.

Minnis, P., D. F. Young, B. A. Wielicki, P. W. Heck, X. Dong, L. L. Stowe, R. Welch, 1999b: CERES cloud properties derived from multispectral VIRS data. *Proc. The EOS/SPIE Symposium on Remote Sensing*, **Vol. 3867**, Florence, Italy, September 20-24, 91-102.

Minnis, P. and B. A. Wielicki, 1988: Comparison of cloud amounts using GOES and Landsat data. *J. Geophys. Res.*, **93**, 9385-9403.

Nguyen, L., P. Minnis, J. K. Ayers, W. L. Smith, Jr., and S. P. Ho, 1999: Intercalibration of geostationary and polar satellite data using AVHRR, VIRS, and ATSR-2 data. *Proc. AMS 10th Conf. Atmos. Rad.*, Madison, WI, June 28 – July 2, 405-408.

Rossow, W. B., A. W. Walker, and L. C. Garder, 1993: Comparison of ISCCP and other cloud amounts. *J. Climate*, **6**, 2394-2418.

Schreiner, A. J., D. A. Unger, W. P. Menzel, G. P. Ellrod, K. I. Strabala, and J. L. Pellet, 1993: A comparison of ground and satellite observations of cloud cover. *Bull. Amer. Meteor. Soc.*, **74**, 1851-1861.

Sherr, P.E., A. H. Glaser, J. C. Barnes, and J. H. Willand, 1968: World-wide cloud cover distributions for use in computer simulations. NASA CR-61226, NASA Marshall Space Flight Center.

Trepte, Q., Y. Chen, S. Sun-Mack, P. Minnis, D. F. Young, B. A. Baum, and P. W. Heck, 1999: Scene identification for the CERES cloud analysis subsystem. *Proc. AMS 10th Conf. Atmos. Rad.*, Madison, WI, June 28 – July 2, 169-172.

Wielicki, B. A. and L. Parker, 1992: On the determination of cloud cover from satellite sensors: The effect of sensor spatial resolution. *J. Geophys. Res.*, **97**, 12,799-12,823

4.1.8 Tables

Table 1: GLOBAL CLOUD CLIMATOLOGIES

Region	Description	Location	Seasonal Change in Cloud Amt	Dominant Cloud Type	Diurnal Variation in Cloud Amt
01	Essentially Clear	Major Desert Area	Small	-----	Small
02	Little Cloudiness	Sub-Desert Area	Small	-----	Small
03	Tropical Cloudy	Near Equator	Small	Convective	Large

Table 1: GLOBAL CLOUD CLIMATOLOGIES

Region	Description	Location	Seasonal Change in Cloud Amt	Dominant Cloud Type	Diurnal Variation in Cloud Amt
04	Tropical Moderate Cloudiness	N or S of Region 3	Small	Convective	Large
05	Desert Marine	Over Ocean off W. Coast	Small	Stratiform	Large
06	Desert Marine Cloudy Winter	Over Ocean W. of Peru	Extreme	Stratiform	Large
07	Desert Marine Cloudy Summer	Over Ocean W. of Baja Calif.	Extreme	Stratiform	Large
08	Mid-latitude Clear Summer	North America	Extreme	Synoptic Scale	Small
09	Mid-Latitude Cloudy Summer	North America & Asia	Moderate	Synoptic Scale	Small
10	High Latitude Clear Winter	Asia & North America	Extreme	Synoptic Scale	Small
11	Mid-Latitude Land	Northern Hemisphere	Moderate	Synoptic Scale	Small
12	Tropical CLoudy Summer	North of Region 3	Moderate	Convective	Large
13	Mid-Latitude Ocean	Northern Hemisphere	Moderate	Synoptic Scale	Small

Table 1: GLOBAL CLOUD CLIMATOLOGIES

Region	Description	Location	Seasonal Change in Cloud Amt	Dominant Cloud Type	Diurnal Variation in Cloud Amt
14	High Latitude Ocean	Northern Hemisphere	Moderate	Synoptic Scale	Small
15	Polar	Northern Hemisphere	Small	Synoptic Scale	Small
16	Tropical Seasonal Change	North of Region 3	Extreme	Convective	Large
17	Tropical Clear Winter	Northern Hemi-sphere near Region 16	Moderate	Convective	Large
18	Mediterra-nean	Northern Hemi-sphere Europe, West North America	Extreme	Convective	Small
19	Sub-Tropical	Northern Hemi-sphere ~30N	Moderate	Convective Synoptic Scale	Large
20	Sub-Tropical Ocean	Northern Hemi-sphere ~30N	Moderate	Convective Synoptic Scale	Small
21	Tropical Cloudy Summer	South of Region 3	Moderate	Convective	Large
22	Mid-Latitude Ocean	Southern Hemisphere	Moderate	Synoptic Scale	Small
23	High Latitude Ocean	Southern Hemisphere	Moderate	Synoptic Scale	Small

Table 1: GLOBAL CLOUD CLIMATOLOGIES

Region	Description	Location	Seasonal Change in Cloud Amt	Dominant Cloud Type	Diurnal Variation in Cloud Amt
24	Polar	Southern Hemisphere	Small	Synoptic Scale	Small
25	Tropical Seasonal Change	South of Region 3	Extreme	Convective	Large
26	Tropical Clear Winter	South of Region 25 Africa Australia	Moderate	Convective	Large
27	Mediterra-nean	Southern Hemisphere Australia Chile	Extreme	Convective	Small
28	Sub-Tropical Land	Southern Hemisphere ~30S	Moderate	Convective Synoptic Scale	Large
29	Sub-Tropical Ocean	Southern Hemisphere ~30S	Moderate	Convective Synoptic Scale	Small

Table 2: Cloud Validation Sites

Cloud Site Index	Description - see Measurement Category Codes in Table 7	Elev (m)	Latitude	Longitude (-180 .. 180)	CERES 1-deg Region Number (Nested)	Validation Region Index
1	Cape Verde	0	16.5000	-22.5000	26438	1
2	Sub-Saharan Africa	427	13.1245	19.9286	27560	2
3	SW Africa coast (south)	1524	-21.8741	16.8600	40157	3
4	S. Greenland Coast	671	60.6210	-47.2340	10573	4
5	US/Canada Pacific Coast	0	48.1225	-132.1875	14807	5
6	Rockies	1402	41.8730	-115.2336	17345	6
7	ARM Site Okla. - F,A,M,SKY,TQ,MW,cr,cl	305	36.6100	-97.4900	19163	7
8	Gulf Stream	0	33.1235	-72.4481	20268	8
9	Bermuda	0	34.0000	-64.5000	19916	9
10	Dry Tortugas	0	24.6000	-82.8000	23498	10
11	Peru Coast	0	-6.8747	-82.4475	34658	11
12	Brazil (north)	244	8.0000	-61.9149	29279	12
13	Brazil (south)	305	-8.1247	-53.6842	35407	13
14	Siberia	152	56.8715	88.2803	12149	14
15	Taklimakan Desert	1372	38.1232	78.5022	18619	15
16	Tibet	4877	35.0000	90.0000	19711	16
17	Middle East	640	28.1238	43.2284	22184	17
18	SE Asia	457	13.1245	108.6429	27649	18
19	Male Is. (Indian)	0	4.1800	73.5200	30854	19
20	Australia/Indonesia (north)	0	0.6250	136.8750	32357	20
21	Australia/Indonesia (south)	0	-20.6241	154.0000	39935	21
22	Cape Grim	0	-41.0000	144.0000	47125	22
23	Azores	0	43.1229	-24.8571	16716	23
24	Barbados	0	13.2000	-59.5000	27481	24
25	Pacific ITCZ	0	3.1249	-149.3750	30991	25
26	Florida, Coasts	30	29.0000	-82.0000	21699	26

Table 2: Cloud Validation Sites

Cloud Site Index	Description - see Measurement Category Codes in Table 7	Elev (m)	Latitude	Longitude (-180 .. 180)	CERES 1-deg Region Number (Nested)	Validation Region Index
27	Tropical Western Pacific - f,a,m,sky,tq,mw,cr,	0	-2.0600	147.4200	33448	27
28	Nauru Island (ARM TWP2) - f,a,m,sky,tq,mw,cr,c	0	-0.5210	166.9160	32747	28
29	ARM Site Alaska - F,A,M,SKY,TQ,MW,CR,CL	0	71.3000	203.3280	6501	29
30	Mexico	0	20.5000	278.5000	24939	30